Theory of the inverse hook method for measuring oscillator strengths

W. A. van Wijngaarden, K. D. Bonin, and W. Happer
Department of Physics, Princeton University, Princeton, New Jersey 08544
(Received 10 October 1986; revised manuscript received 16 March 1987)

The theory of a new method to measure oscillator strengths is presented. The method exploits the ac Stark interaction of a laser pulse detuned from a transition between an initially populated state a and a second state b of an atom. We assume the density matrix ρ of state a initially has only diagonal elements given by $\langle m|\rho|m\rangle = C + Dm^2$ where C and $D \neq 0$ are constants and m is the Zeeman sublevel quantum number. The laser pulse is linearly polarized along an axis different from the quantization axis and therefore rearranges the atoms among the various Zeeman sublevels. Changes of the relative Zeeman sublevel populations induced by the laser pulse can be readily detected by monitoring changes in the angular distribution or polarization of fluorescent light emitted when the atoms radiatively decay to some final state f. This paper considers the general problem where states a, b, and f have arbitrary angular momentum. We derive the functional dependence of the polarized fluorescent light fluence on the laser pulse fluence (pulse energy per unit area). For spatially uniform laser pulses, these signals are periodic functions of the laser fluence. When the laser is completely speckled, we show that the signal is well approximated by a Lorentzian curve. This latter case is of considerable experimental interest since most pulsed dye lasers have poor transverse mode structure which can readily be converted into a statistically well-defined speckle pattern. The oscillator strength of the transition between states a and b is found using (1) the fluence half-width of the "depolarization curve," the Lorentzian-like dependence of the fluorescence polarization on the laser pulse fluence, (2) the detuning of the laser from the transition frequency ω_{ab}, and (3) some known constant factors which depend on the angular momenta of states a, b, and f. The physics of the situation is very similar to that of the conventional hook method with this difference: the roles of the atoms and the photons have been interchanged. We therefore call this new method *the inverse hook method.* The inverse hook method is relatively insensitive to the details of the atomic absorption line shape and also to the temporal and spatial profile of the laser pulse. It yields absolute oscillator strengths and it is especially suitable for measurements of transitions between excited atomic states, including autoionizing states.

I. INTRODUCTION

Oscillator strengths or absolute atomic transition probabilities are needed for such different problems as the determination of the constituent concentrations of stellar matter[1] and the optimization of isotope separation by selective laser ionization.[2-4] There are several different definitions of oscillator strength in the literature.[5-8] We shall use Corney's definition of an oscillator strength f_{ab} for a transition from an initial level a to a final level b,

$$f_{ab} = \frac{2m_e\omega_{ba}}{3\hbar e^2[J_a]} \sum_{m_b,m_a} |\langle am_a|\mathbf{D}|bm_b\rangle|^2 , \quad (1)$$

where m_e is the electron mass, e is the electron charge, $\omega_{ba} = (E_b - E_a)/\hbar$, where E_a and E_b are the energies of levels a and b, $[J] = 2J+1$ is the statistical weight of a level with electronic angular momentum J, m is the azimuthal quantum number, and the electric dipole moment operator is $\mathbf{D} = e\sum_n \mathbf{r}_n$, where $\mathbf{r}_n$ is the position vector of the nth atomic electron.

A number of methods have been developed to measure oscillator strengths.[9-14] Unfortunately, as is discussed in the excellent review article by Huber and Sanderman,[9] it remains especially difficult to determine oscillator strengths for transitions between excited states. This paper discusses a new method called the inverse hook method which was specifically designed to determine oscillator strengths for such transitions. It has been used to measure oscillator strengths in rubidium for the $nD_{3/2} \rightarrow 5P_{3/2}, 5P_{1/2}$ $n = 6,7$ transitions.[15]

We shall begin by giving a brief description of the inverse hook method. A schematic sketch of the experimental apparatus is shown in Fig. 1. Two laser pulses of different frequencies are used. The first or "exciting" pulse, EXC of Fig. 1, propagates along the y axis and is linearly polarized along the z axis of a coordinate system. In the experiment described in Ref. 15, this laser excited the rubidium atoms from the ground state to the $6D_{3/2}$ or $7D_{3/2}$ level via a two-photon excitation. This initial excited state is called the populated level and denoted by a. It is essential that the exciting pulse produce an anisotropic distribution of atoms among the sublevels of a as illustrated in Fig. 2(a).

Shortly after the atoms are excited and before there has been appreciable spontaneous decay, a second pulse of

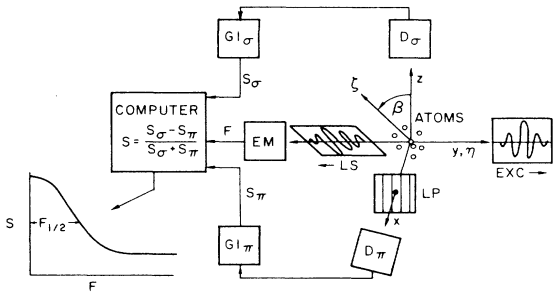

FIG. 1. Basic experimental arrangement. The laser pulses are shown just after they have passed through the atomic vapor. The atoms are first excited by laser pulse EXC. Later a light shift (LS) laser pulse from a second dye laser perturbs the atoms as discussed in the text and illustrated in Fig. 2. An energy meter EM measures the energy of the LS pulse and sends this reading to a computer. Unpolarized and linear polarized fluorescence are detected by detectors D_σ and D_π. The fluorescent signals are input to gated integrators GI_σ and GI_π whose outputs S_σ and S_π are also transmitted to the computer. Finally, the computer analyzes the data and plots it as shown in the figure.

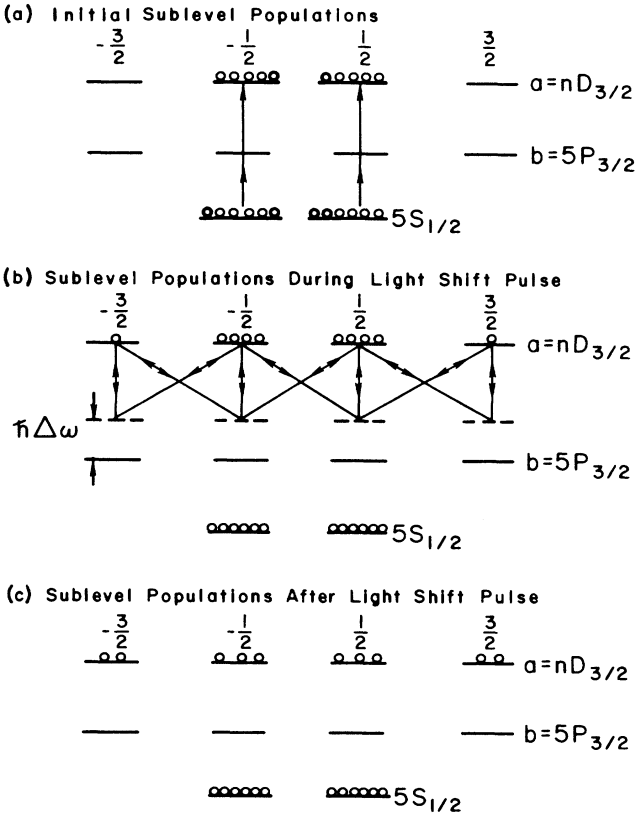

FIG. 2. Zeeman sublevel populations during the experiment. Initially, a state a is excited in such a way that all the sublevels of a are not equally populated. This is illustrated in (a), where only the $m_J = \pm\frac{1}{2}$ sublevels of a are populated by a two-photon excitation from the ground state. Next, as shown in (b), the atoms are subject to the ac Stark shift of a laser pulse detuned from a transition between states a and b. The atoms are redistributed among the sublevels of a since the light shift laser is linearly polarized along a direction different from the quantization axis.

laser light propagates through the atoms along the negative y axis. The frequency ω of the second or "light shift" laser is tuned close to but not equal to the resonant frequency $|\omega_{ab}|$ of the transition from level a to level b for which the oscillator strength is to be measured. The light shift pulse is linearly polarized along a direction $\hat{\zeta}$ which is tilted by an angle β from the z axis and which lies in the xz plane as shown in Fig. 1. The effect of the light shift pulse on the atoms is illustrated in Fig. 2(b). The light causes virtual transitions from sublevels of a to sublevels of b and back to different sublevels of a. After the light shift pulse, the distribution of population in the sublevels of a will have been modified as indicated in Fig. 2(c).

The changes in sublevel populations caused by the light shift laser are measured by observing changes in the fluorescence polarization emitted when the excited atoms radiatively decay to a final state f. The fluorescence polarization signal is measured for many different light shift pulse fluences (pulse energy per unit area) and is plotted as shown in Fig. 1. In this paper we shall show how the oscillator strength for the transition between states a and b can be found using

(1) the fluence half-width of the "depolarization curve," the Lorentzian-like dependence of the fluorescence polarization on the laser pulse fluence,

(2) the detuning of the laser from the transition frequency ω_{ab}, and

(3) some known constant factors which depend on the angular momenta of states a, b, and f.

This problem has not been solved previously, except for the special case of transitions between a $D_{3/2}$ populated state and a $P_{3/2}$ or $P_{1/2}$ state.[15] In this paper a detailed account of the theory of the inverse hook method is presented for the general case where states a, b, and f have arbitrary angular momentum. The basic result of the paper is Eq. (78). The depolarization curve has a width $F_{1/2}$ which is inversely proportional to the oscillator strengths, with constants of proportionality which are given in Table I and Eq. (19).

II. THEORY

We begin by considering the response of an excited atom to the electric field of the light shift laser, which we write as

$$\mathbf{E} = \mathcal{E} e^{-i\omega t} + \mathcal{E}^* e^{i\omega t} . \tag{2}$$

The field amplitude $\mathcal{E}$ is a function of time which varies slowly with respect to the laser frequency ω. For example, $\mathcal{E}$ will typically be a pulse envelope which rises and falls in a few nanoseconds. The interaction of the electric dipole moment $\mathbf{D}$ of the atom and the electric field of the light is

$$V = -\mathbf{D}\cdot\mathbf{E} . \tag{3}$$

TABLE I. Half-width parameter $\theta_{1/2}$ and residual polarization parameter ϵ.

J_a	ϵ	$\theta_{1/2}$	J_a	ϵ	$\theta_{1/2}$
1	0.3333	1.000	$\frac{3}{2}$	0	1.000
2	0.1429	1.031	$\frac{5}{2}$	0	1.260
3	0.0952	1.190	$\frac{7}{2}$	0	1.377
4	0.0722	1.297	$\frac{9}{2}$	0	1.444
5	0.0582	1.369	$\frac{11}{2}$	0	1.492
6	0.0490	1.423	$\frac{13}{2}$	0	1.526
7	0.0422	1.463	$\frac{15}{2}$	0	1.551
8	0.0372	1.493	$\frac{17}{2}$	0	1.573
9	0.0332	1.519	$\frac{19}{2}$	0	1.591
10	0.0300	1.539	$\frac{21}{2}$	0	1.603
∞	0	1.753	∞	0	1.753

We shall consider excited atoms in an initially populated level a like that of Fig. 2. We suppose that the level has electronic angular momentum J_a and that the hyperfine structure can be ignored. As we mentioned in connection with our earlier discussion of Fig. 2(b), the frequency of the light shift laser is sufficiently detuned from resonance so that it can only transfer atoms between the sublevels $|m\rangle$ of level a. We assume that these sublevels are quantized along the z axis of Fig. 1. The azimuthal quantum number m is thus defined by

$$J_z|m\rangle = m|m\rangle \ , \tag{4}$$

where J_z is the projection of the electronic angular momentum operator along the z direction. We denote the probability amplitudes of the sublevels $|m\rangle$ by $c(m)$. The coupling of these amplitudes by the light shift laser [i.e., by the virtual transitions sketched in Fig. 2(b)] is described by the interaction-picture differential equation

$$i\hbar\dot{c}(m) = \sum_{m'} \langle am|H|am'\rangle c(m') \ . \tag{5}$$

We assume that the light shift pulse is of such short duration that coupling terms due to hyperfine structure, magnetic fields, etc., can be neglected. The matrix elements $\langle m|H|m'\rangle$ of (5) are given by second-order perturbation theory applied to the interaction (3), i.e.,

$$\langle m|H|m'\rangle = -\sum_{\mu,b} \frac{\langle am|\mathcal{E}\cdot\mathbf{D}|b\mu\rangle\langle b\mu|\mathcal{E}^*\cdot\mathbf{D}|am'\rangle}{\hbar(\omega_{ba}+\omega)} - \sum_{\mu,b} \frac{\langle am|\mathcal{E}^*\cdot\mathbf{D}|b\mu\rangle\langle b\mu|\mathcal{E}\cdot\mathbf{D}|am'\rangle}{\hbar(\omega_{ba}-\omega)} \ . \tag{6}$$

The denominators contain the Bohr frequencies

$$\omega_{ba} = \frac{E_b - E_a}{\hbar} \tag{7}$$

for transitions between level b with energy E_b and level a with energy E_a.

The interaction (3) has odd parity and therefore cannot couple $|m\rangle$ and $|m'\rangle$ in first order or in any odd order of perturbation theory. The perturbation expansion parameter is $(\omega_R/\Delta\omega)^2$ where $\omega_R \approx \mathcal{E}D_{ab}$ is the Rabi frequency, and $\Delta\omega = \omega - |\omega_{ab}|$ is the detuning frequency. We assume that no higher-order coupling terms in addition to the second-order terms of (6) are needed.

The first term on the right of (6) describes a virtual transition from sublevel $|am'\rangle$ to sublevel $|b\mu\rangle$ with the creation by $\mathcal{E}^*$ of a photon of energy $\hbar\omega$, followed by a transition from $|b\mu\rangle$ to $|am\rangle$ with reabsorption of the photon. The second term on the right of (6) describes a similar process in which a photon is first absorbed and then recreated. Since we assume that $\omega \approx |\omega_{ba}|$, one of the energy denominators of (6) will be very small compared to the other, and the term associated with the small energy denominator will make almost all of the contribution to $\langle m|H|m'\rangle$. This dominant term corresponds to creation and destruction of photons in an order which nearly conserves energy for the virtual transitions.

We shall consider the special case of laser light which is linearly polarized along the ζ axis of the "tilted" coordinate system $\xi\eta\zeta$ of Fig. 1. The electric field amplitudes of (2) can be written as

$$\mathcal{E} = \mathcal{E}\hat{\zeta} \ , \tag{8}$$

where $\hat{\zeta}$ is a unit vector along the ζ axis. The Hamiltonian matrix $\langle m|H|m'\rangle$ of (6) can be diagonalized if we choose basis states $|m\}$ for level a which are quantized along the direction $\hat{\zeta}$, i.e.,

$$J_\zeta|m\} = m|m\} \ , \tag{9}$$

where $J_\zeta = \hat{\zeta}\cdot\mathbf{J}$. We shall use curly kets $|m\}$ to distinguish sublevels quantized along $\hat{\zeta}$ from sublevels $|m\rangle$ quantized along $\hat{\mathbf{z}}$.

The Hamiltonian (6) can now be written as

$$H = -\mathcal{E}^2 \sum_m \alpha(m)|am\}\{am| \ . \tag{10}$$

The polarizability $\alpha(m)$ of the state $|m\}$ can be calculat-

ed from (6) by means of the Wigner-Eckart theorem and the definition (1) of the oscillator strength to be

$$\alpha(m)=\sum_b \frac{3e^2 f_{ab}}{m_e(\omega_{ab}^2-\omega^2)} C^2(J_b,1,J_a;m,0) \ . \tag{11}$$

The relevant Clebsch-Gordan coefficients are

$$\begin{aligned} C^2(J_a+1,1,J_a;m,0)&=\frac{(J_a+1)^2-m^2}{(J_a+1)(2J_a+3)} \ , \\ C^2(J_a,1,J_a;m,0)&=\frac{m^2}{J_a(J_a+1)} \ , \\ C^2(J_a-1,1,J_a;m,0)&=\frac{J_a^2-m^2}{J_a(2J_a-1)} \ . \end{aligned} \tag{12}$$

The evolution of the sublevel amplitudes $c(m)$ due to the light shift laser, i.e., the solution of (5) is

$$c_f(m)=\sum_{m'} \langle m \mid U \mid m' \rangle c_i(m') \ , \tag{13}$$

where the sublevel amplitudes before and after the light shift pulse have been denoted by the subscripts i and f. The time evolution operator is

$$U=\exp\left[\frac{-i}{\hbar}\int_{t_i}^{t_f} H\,dt\right]=\sum_m e^{-i\phi(m)} \mid m \rangle\langle m \mid \ . \tag{14}$$

The phases follow from (10) and are

$$\phi(m)=-\frac{2\pi\alpha(m)}{c\hbar}F \ . \tag{15}$$

The fluence F is related to the laser intensity I

$$I=\frac{c\mathcal{E}^2}{2\pi} \tag{16}$$

by

$$F=\int_{t_i}^{t_f} I\,dt \ . \tag{17}$$

For future reference we note that the phases can be written as

$$\phi(m)=\frac{m^2 F}{(2J_a-1)\Delta F}+\phi_0 \ , \tag{18}$$

where ϕ_0 is independent of m. The parameter ΔF is given by

$$\frac{1}{\Delta F}=\frac{6\pi e^2}{m_e c\hbar}\sum_b \frac{\kappa_{ab} f_{ab}}{\omega_{ab}^2-\omega^2} \ . \tag{19}$$

The coefficients κ_{ab} follow from (12) and are

$$\kappa_{ab}=\begin{cases} \dfrac{2J_a-1}{(J_a+1)(2J_a+3)} & \text{if } J_b=J_a+1 \\ -\dfrac{2J_a-1}{J_a(J_a+1)} & \text{if } J_b=J_a \\ \dfrac{1}{J_a} & \text{if } J_b=J_a-1 \ . \end{cases} \tag{20}$$

There is an interesting physical meaning to (14) which will help to clarify the significance of the inverse hook method. According to the correspondence principle of quantum mechanics, atoms in a superposition of the adjacent azimuthal quantum states $\mid m \}$ and $\mid m-1 \}$ will rotate about the ζ axis at a rate

$$\omega_m=\frac{d}{dt}[\phi(m)-\phi(m-1)]=\frac{2m-1}{2J_a-1}\frac{I}{\Delta F} \ . \tag{21}$$

The total rotation angle of the atoms is

$$\int \omega_m\,dt=\frac{2m-1}{2J_a-1}\theta \ , \tag{22}$$

where the characteristic twist angle is

$$\theta=\frac{F}{\Delta F} \ . \tag{23}$$

From (22) and (23) we see that $\mid \Delta F \mid$ is the laser pulse fluence needed to rotate atoms with their spins "pointing north" (i.e., atoms with $m=J_a$) by 1 rad. The sign of the rotation angle is the same as the sign of ΔF. Atoms with their spins pointing south (i.e., atoms with $m=-J_a+1$) will rotate by 1 rad in the opposite direction. The linearly polarized light shift laser *twists* the atomic spin distribution uniformly about the polarization of the light. We may therefore call the unitary operator U of (14) a *torison operator*. We shall consider the properties of this operator in more detail later.

Since we shall be dealing with ensembles of atoms, it will be more convenient to describe the atoms with a density matrix $\langle m \mid \rho \mid m' \rangle$ instead of the state amplitudes $c(m)$ of (4). These quantities are related by

$$\langle m \mid \rho \mid m' \rangle=\langle c(m)c^*(m') \rangle_{\text{av}} \ , \tag{24}$$

where the subscript av denotes an averaging of the amplitude products over all atoms of the ensemble. We denote the initial density matrix which describes the atoms in level a before the light shift pulse by ρ_i. After the light shift pulse has caused the changes indicated in Fig. 2, the atoms in state a will be described by the final density matrix ρ_f.

$$\rho_f=U\rho_i U^\dagger \ , \tag{25}$$

where U was given by (14).

To proceed further we must specify the form of the initial density matrix. We shall assume that before the light shift pulse the atoms have pure alignment polarization, i.e., the populations of the sublevels $\mid m \rangle$ are given by

$$\langle m \mid \rho_i \mid m \rangle=C+Dm^2 \ , \tag{26}$$

where C and D are constants.[16] We also assume that ρ_i has no off-diagonal matrix elements between the basis states $\mid m \rangle$. Purely aligned atoms are produced when linearly polarized light is used to excite atoms from an unpolarized ground state. Different initial polarizations can be produced if the atoms are excited with circularly polarized light (both orientation and alignment can be generated), if the atoms are excited from a polarized ground state or if multipole quantum transitions are used to excite the atoms with linearly polarized light into a level with electronic angular momentum $J_a \geq 2$. However, the case of pure alignment is so common that we shall

focus on it for the remainder of the paper. The situation for other initial polarizations can be analyzed in a way similar to that outlined below.

Further calculations will be simplified if we describe the initially aligned state with irreducible tensor basis operators, i.e., we rewrite (26) as

$$\rho_i = A_0 + A_2 T_{20} , \tag{27}$$

where the constants A_0 and A_2 are linear combinations of the constants C and D. The tensor is defined by

$$T_{LM} = \sum_m | Jm \rangle \langle Jm-M | (-1)^{m-M-J} \times C(J,J,L;m,M-m) , \tag{28}$$

where the bra and ket vectors are understood to be quantized along the z axis of Fig. 1. We shall make frequent use of the orthonormality of the unit tensors.

$$\mathrm{Tr}(T_{LM} T^{\dagger}_{L'M'}) = \delta_{LL'}\delta_{MM'} . \tag{29}$$

Substituting (27) into (25) we find

$$\rho_f = A_0 + A_2 U T_{20} U^{\dagger} . \tag{30}$$

Since U is most conveniently expressed in terms of the tilted basis states $| m \}$, c.f. (14), we shall express T_{20} in the same basis. From Fig. 1 we see that

$$| m \} = R | m \rangle \tag{31a}$$

or

$$| m \rangle = R^{\dagger} | m \} , \tag{31b}$$

where the rotation operator is

$$R = e^{-i\beta J_y} = e^{-i\beta J_\eta} . \tag{32}$$

We denote irreducible basis tensors in the tilted coordinate system, in analogy to (28), by

$$\mathcal{T}_{LM} = \sum_m | Jm \} \{ Jm-M | (-1)^{m-M-J} \times C(J,J,L;m,M-m) . \tag{33}$$

Comparing (28), i.e., (31), and (33), we see that[17]

$$T_{LM} = R^{\dagger} \mathcal{T}_{LM} R = \sum_{M'} \mathcal{T}_{LM'} d^L_{M'M}(-\beta) , \tag{34}$$

where $d^L_{M'M}(-\beta)$ is the Wigner function for the special case of a rotation by an angle $-\beta$ about the y or η axis. Substituting (34) into (30) we find

$$\rho_f = A_0 + A_2 \sum_M U \mathcal{T}_{2M} U^{\dagger} d^2_{M0}(-\beta) . \tag{35}$$

From (14) and (33), we find that the quantity $U\mathcal{T}_{2M}U^{\dagger}$ which appears in (34) can be written as

$$U \mathcal{T}_{2M} U^{\dagger} = \sum_L \mathcal{T}_{LM} v^{L2}_M , \tag{36}$$

where the torison matrix is

$$v^{LL'}_M = \sum_m C(J_a,J_a,L;m,M-m) C(J_a,J_a,L';m,M-m) \times e^{i[\phi(m-M)-\phi(m)]} . \tag{37}$$

In deriving (36) we made use of the inverse of (33)

$$| Jm \} \{ Jm-M | (-1)^{m-M-J} = \sum_L \mathcal{T}_{LM} C(J,J,L;m,M-m) . \tag{38}$$

The torsion matrix (37) has an important significance in the analysis of inverse hook experiments. According to (36), the light shift laser transforms a tensor $\mathcal{T}_{2M}$ quantized along the direction of linear polarization of $\hat{\xi}$ into a superposition of tensors of the same azimuthal quantum number M but different multipole indexes L. Physically, the mixing of multipole moments occurs because the light shift laser carriers out a torsional operation on the polarization of the excited state, as we mentioned in connection with our discussion of (21) and (22).

For future reference we now discuss some of the more important properties of the torsion matrix (37). We replace the summation index m of (37) by the mean index

$$q = m - \frac{M}{2} , \tag{39}$$

and we note from (18) and (23) that the phase difference of (37) is

$$\phi(m-M) - \phi(m) = -\frac{2qM\theta}{2J_a - 1} . \tag{40}$$

Then (37) becomes

$$v^{LL'}_M(\theta) = \sum_q C\left[J_a,J_a,L;\frac{M}{2}+q,\frac{M}{2}-q \right] \times C\left[J_a,J_a,L';\frac{M}{2}+q,\frac{M}{2}-q \right] \times \exp\left[\frac{-iqM\theta}{J_a - \frac{1}{2}} \right] . \tag{41}$$

One can show that $v^{LL'}_M(\theta)$ are either pure imaginary or real functions. According to (39), q can be an integer or a half-integer summation index, depending on M and on whether m (i.e., J_a) is an integer or a half-integer. Note that the torsional coefficients are periodic in the fluence angle θ.

We substitute (36) into (35) and use the inverse of (34)

$$\mathcal{T}_{LM} = \sum_{M'} T_{LM'} d^L_{M'M}(\beta) \tag{42}$$

to write

$$\rho_f = A_0 + A_2 \sum_{L,M} T_{LM} V^{L2}_{M0} , \tag{43}$$

where the torsion matrix in the xyz coordinate system is

$$V^{LL'}_{MM'}(\theta,\beta) = \sum_{M''} d^L_{MM''}(\beta) v^{LL'}_{M''}(\theta) d^{L'}_{M''M'}(-\beta) . \tag{44}$$

The torsion matrices $V^{LL'}_{MM'}(\theta,\beta)$ have the same

significance in the xyz coordinate system as the matrices $v_M^{LL'}(\theta)$ in the $\xi\eta\zeta$ system. The analog of (36) is

$$UT_{L'M'}U^{\dagger}=\sum_{L,M} T_{LM}V_{MM'}^{LL'} . \tag{45}$$

The torsion matrices V have a number of symmetry properties which for the sake of brevity we shall not discuss.

So far we have ignored the possibility that the excited atoms may have hyperfine structure or that an external magnetic field $H_{\rm mag}$ may be present. We now generalize our discussion slightly by assuming that a magnetic field is directed along the z axis. The field is small enough that it causes negligible precession during the short time interval of the light shift pulse, but it is big enough to decouple any small hyperfine structure like that of the higher excited D states of the alkali-metal atoms. A more quantitative discussion of the effects of the magnetic field during the light shift pulse is given at the end of this section. The decoupling of the electronic polarization from the nuclear polarization is advantageous in an experiment since it increases the polarization of the fluorescent light by preventing electronic polarization from being transformed to nuclear polarization. Decoupling also simplifies the theoretical analysis since it allows one to ignore the nucleus. The previous calculations then remain valid except that they must be augmented by considering the precession of the electronic polarization at the frequency

$$\Omega=\frac{g_J\mu_B H+A_J m_I}{\hbar} , \tag{46}$$

where m_I is the projection of the nuclear spin on the z axis, A_J is the magnetic dipole hyperfine constant, g_J is the electronic g factor of level a, and μ_B is the Bohr magneton. We have assumed that the electric quadrupole hyperfine interaction is negligible. Because the initially excited atoms have a polarization which is axially symmetric about the magnetic field [cf. (27)], the magnetic field will have no effect on the atomic polarization until after the light shift laser has suddenly created various components of transverse polarization T_{LM} $(M\neq 0)$ in accordance with (43). The newly generated transverse polarization components will rotate at the Larmor frequency of the excited atoms so the density matrix (43) becomes

$$\rho_f=A_0+A_2\sum_{L,M} e^{-iM\Omega t}T_{LM}V_{M0}^{L2} , \tag{47}$$

where the time t is measured from the end of the light shift pulse.

The population changes caused by the light shift laser (see Fig. 2) can be detected by observing resulting changes in the polarization or angular distribution of fluorescent light, as indicated in Fig. 1. The power P of fluorescent light reaching the detector is given by[18]

$$P=Ne^{-t/\tau_a}\mathrm{Tr}(\mathcal{L}\rho_f) , \tag{48}$$

where τ_a is the natural lifetime of the fluorescing atoms in level a, and N is an overall constant which accounts for the number of excited atoms, the solid angle subtended by the detector, and the transmission efficiency of the filters and polarizers, etc. The fluorescent light operator $\mathcal{L}$ describes how much fluorescent light will reach the detector through the polarization analyzing devices placed between the fluorescing atoms and the detector. For the case of polarization analyzer which passes light linearly polarized along the unit vector $\hat{\mathbf{u}}$, we can write

$$\mathcal{L}=B_0+B_2\sum_M Y_{2M}(\hat{\mathbf{u}})T_{2M}^{\dagger} . \tag{49}$$

As was shown in Ref. 18, the coefficients B_0 and B_2 depend on the electronic angular momentum J_a of the excited atom and the angular momentum J_f of the level in which the atom is left after emission of a fluorescent photon. The tensor T_{2M} was defined in (28) and $Y_{2M}(\hat{\mathbf{u}})$ is the value of the spherical harmonic at the location $\hat{\mathbf{u}}$ on the unit sphere.

Substituting (47) and (49) into (48), we find that the fluorescent power is given by the following:

$$P(\hat{\mathbf{u}})=Ne^{-t/\tau_a}\left[A_0B_0[J_a]+A_2B_2\sum_M e^{-iM\Omega t}Y_{2M}V_{M0}^{22}\right] . \tag{50}$$

We note that the fluorescent power damps at the natural decay rate τ_a^{-1} of the level a and it exhibits the light beats of Dodd and Series[19] at the Larmor frequency Ω and its second harmonic 2Ω.

For inverse hook measurements, we integrate the fluorescent power for several natural lifetimes as indicated in Fig. 1 to obtain a fluorescent signal

$$S(\hat{\mathbf{u}})\approx G\int_0^{\infty}P(\hat{\mathbf{u}})dt=1+\frac{AB}{2}\left[\frac{4\pi}{5}\right]^{1/2}\sum_M\frac{Y_{2M}(\hat{\mathbf{u}})V_{M0}^{22}}{1+iM\Omega\tau_a} , \tag{51}$$

where G is a gain coefficient chosen for convenience to make the polarization-independent part of the signal unity. The initial alignment coefficient A is

$$A=\frac{A_2}{A_0[J_a]} , \tag{52}$$

and the branching sensitivity coefficient is

$$B=2\left[\frac{5}{4\pi}\right]^{1/2}\frac{B_2}{B_0} . \tag{53}$$

We shall discuss the coefficients A and B in more detail later.

Let us consider the signals (51) for fluorescence linearly polarized along the three coordinate axes x, y, and z. We know that

$$Y_{2M}(\hat{\mathbf{z}})=\delta_{M0}\left[\frac{5}{4\pi}\right]^{1/2} . \tag{54}$$

Substituting (54) into (51) we find

$$S(\hat{\mathbf{z}})=S_{\pi}=1+\frac{AB}{2}V_{00}^{22} . \tag{55}$$

As indicated in (55), $S(\hat{\mathbf{z}})$ is the same as the π signal of Fig. 1.

We now consider (51) when $\hat{\mathbf{u}}=\hat{\mathbf{x}}$. We know that

$$Y_{2M}(\hat{\mathbf{x}})=-\frac{\delta_{M0}}{2}\left[\frac{5}{4\pi}\right]^{1/2}+\left[\frac{15}{32\pi}\right]^{1/2}(\delta_{2M}+\delta_{-2M}) . \tag{56}$$

Substituting (56) into (51), and using the fact that $V_{-20}=V_{20}$, we find

$$S(\hat{\mathbf{x}})=1-\frac{AB}{4}V_{00}^{2}+AB\left[\frac{3}{8}\right]^{1/2}V_{20}^{22}\frac{1}{1+(2\Omega\tau_a)^2} . \tag{57}$$

In like manner we find

$$S(\hat{\mathbf{y}})=1-\frac{AB}{4}V_{00}^{22}-AB\left[\frac{3}{8}\right]^{1/2}V_{20}^{22}\frac{1}{1+(2\Omega\tau_a)^2} . \tag{58}$$

We note that $S(\hat{\mathbf{x}})$, $S(\hat{\mathbf{y}})$, and $S(\hat{\mathbf{z}})$ all contain fluence-dependent terms proportional to V_{00}^{22}. For $S(\hat{\mathbf{x}})$ and $S(\hat{\mathbf{y}})$ there are additional terms containing a product of a fluence-dependent factor V_{20}^{22} and a magnetic depolarization factor (Hanle-effect factor) $[1+(2\Omega\tau_a)^2]^{-1}$. The terms involving the Hanle effect will be negligibly small if the magnetic field is large enough to make $(2\Omega\tau_a)^2\gg 1$. However, these factors are also eliminated by symmetry if, as in the experiment of Fig. 1, the unpolarized fluorescence intensity propagating along the z axis is detected. We then obtain the σ signal of Fig. 1, i.e.,

$$S_\sigma=S(\hat{\mathbf{x}})+S(\hat{\mathbf{y}})=2-\frac{AB}{2}V_{00}^{22} . \tag{59}$$

We see that both the σ and π signals depend on the fluence through the coefficient V_{00}^{22} defined in (44).

Signals like those of (55) and (59) could be generated if a light shift laser with spatially uniform fluence were used in an experiment. Since the signals are superpositions of the torsion coefficients $v_M^{LL'}$ [cf. (41)], they would be periodic functions of the laser fluence. While it is possible in principle to observe such oscillatory signals, it is difficult in practice because pulsed dye lasers usually have poor transverse mode structure. A much more practical experimental procedure is to use a light shift laser for which the spatial distribution of fluence is as inhomogeneous as possible, i.e., a laser with a fully developed speckle distribution.

If the mean fluence of a laser, averaged over many speckles, is F, then the probability of finding a local fluence between F' and $F'+dF'$ is[20–22]

$$P(F')dF'=\frac{e^{-F'/F}}{F}dF' . \tag{60}$$

There will be a distribution of twists experienced by the excited atoms, with atoms in a bright speckle experiencing large twists and atoms in dim speckles experiencing small twits. We may account for the speckled laser beam by replacing the torsion coefficients of (41) by mean torsion coefficients averaged over the distribution (60). These are

$$\bar{v}_M^{LL'}=\sum_q C\left[J_a,J_a,L;\frac{M}{2}+q,\frac{M}{2}-q\right]\times C\left[J_a,J_a,L';\frac{M}{2}+q,\frac{M}{2}-q\right]\frac{1}{1+\dfrac{iqM\theta}{J_a-\frac{1}{2}}} . \tag{61}$$

The mean torsion coefficient for the inverse hook signals [c.f. (55) and (59)] follows from (44) and is

$$\bar{V}_{00}^{22}(\theta,\beta)=\sum_M \bar{v}_M^{22}(\theta)[d_{0M}^{2}(\beta)]^2 . \tag{62}$$

For future reference, we summarize a few useful properties of $\bar{V}_{00}^{22}(\theta,\beta)$. The initial value for zero fluence is

$$\bar{V}_{00}^{22}(0,\beta)=1 . \tag{63}$$

The baseline value at infinite fluence is

$$\bar{V}_{00}^{22}(\infty,\beta)=\frac{(3\cos^2\beta-1)^2}{4}+\frac{9\epsilon}{4}\sin^4\beta , \tag{64}$$

where the parameter ϵ is zero for half-integer J_a and

$$\epsilon=\tfrac{1}{3}C^2(J_a,J_a,2;1,1) \tag{65}$$

for integer J_a. To maximize the fluence-dependent signal one should choose the tilt angle $\beta=\beta_{\text{opt}}$ to minimize $\bar{V}_{00}^{22}(\infty,\beta)$. From (64) we see that

$$\sin^2\beta_{\text{opt}}=\frac{2}{3(1+\epsilon)} . \tag{66}$$

For half-integer J_a where $\epsilon=0$, it follows from (66) that $\beta_{\text{opt}}=54.74°$, the so-called magic angle. For integer values of J_a, β_{opt} is somewhat less than 54.74° because ϵ is a small positive number. For example, if $J_a=1$, we find $\epsilon=\frac{1}{3}$ and $\beta_{\text{opt}}=45°$.

We can readily obtain limiting values of the torsion matrices for $J_a\to\infty$. From algebraic tables of the Clebsch-Gordan coefficients we find as $J_a\to\infty$

$$J_aC^2(J_a,J_a,2;1+q,1-q)\to\tfrac{15}{16}(1-x^2)^2 , \tag{67}$$

where

$$x=\frac{q}{J_a} . \tag{68}$$

From (67), (68), and (61), it follows that the mean torsion coefficient for $J_a\to\infty$ is

$$\bar{v}_2^{22}(\theta)=\tfrac{15}{16}\int_{-1}^{1}(1-x^2)^2\frac{1}{1+(2x\theta)^2}dx . \tag{69}$$

This can be readily evaluated by numerical integration as a function of the relative fluence θ. Similarly, as $J_a\to\infty$

$$J_aC^2(J_a,J_a,2;\tfrac{1}{2}+q,\tfrac{1}{2}-q)\to\tfrac{15}{4}x^2(1-x^2) , \tag{70}$$

so from (68), (70), and (61), we find

$$\bar{v}_1^{22}(\theta)=\tfrac{15}{4}\int_{-1}^{1}\frac{x^2(1-x^2)}{1+(x\theta)^2}dx . \tag{71}$$

We also see from (67) that as $J_a\to\infty$ for integral J_a,

$$\epsilon \rightarrow \frac{5}{16J_a} , \tag{72}$$

so the value of β_{opt} approaches the magic angle for larger integer values of J_a, in accordance with (65) and (66).

Substituting the well-known algebraic expressions for the Wigner functions into (62) we find that

$$\bar{V}^{22}_{00}(\theta,\beta)=\frac{(3\cos^2\beta-1)^2}{4}+\tfrac{3}{4}\sin^2(2\beta)\bar{v}^{22}_{1}(\theta) + \tfrac{3}{4}\sin^4\beta\,\bar{v}^{22}_{2}(\theta) . \tag{73}$$

Using (61) to evaluate $\bar{v}^{22}_{M}(\theta)$ for finite values of J_a and (69) and (71) for the limit $J_a \rightarrow \infty$, we have plotted $\bar{V}^{22}_{00}$ in Figs. 3 and 4 for representative values of J_a and for tilt angle $\beta=54.74°$. The curves fall from an initial value of 1 to a baseline of 0 for half-integer J_a or to the value of ϵ given by (65) for integral J_a. The theoretical half-widths $\theta_{1/2}$ of the curves are given by

$$\bar{V}^{22}_{00}(\theta_{1/2},\beta)=\frac{1+\bar{V}^{22}_{00}(\infty,\beta)}{2} . \tag{74}$$

Equation (74) can be solved numerically to find $\theta_{1/2}(\beta)$. Since $\bar{V}^{22}_{00}$ is an even function of θ, Eq. (74) has two solutions $\pm\theta_{1/2}(\beta)$ where we arbitrarily set $\theta_{1/2}(\beta)>0$. The width parameters $\theta_{1/2}$ for $\beta=54.74°$ are listed in Table I for $J_a \leq 10$. According to (23) the experimental half-width parameter $F_{1/2}$ is related to $\theta_{1/2}$ by

$$F_{1/2}=\theta_{1/2}\,|\,\Delta F\,| . \tag{75}$$

This equation is extremely important since it provides a relation between an experimentally measurable quantity $F_{1/2}$ and a theoretically significant parameter ΔF from which oscillator strengths can be easily inferred with the aid of (19). $F_{1/2}$ will always be a positive quantity since it is the fluence which causes the inverse hook signal to drop from its initial value halfway to its final value as illustrated in Fig. 1. The parameter $|\Delta F|$ in (75) is the fluence needed to cause 1 rad of torsion in the positive or negative sense, in accordance with the sign of ΔF, as discussed in connection with (22) and (23). Although the sign of ΔF cannot be determined from the particular arrangement of the inverse hook method shown in Fig. 1, it can be inferred without ambiguity from the theoretical formula (19) which implies that ΔF changes sign every time the frequency ω of the light shift laser passes through an atomic resonance frequency ω_{ab}. The sign of ΔF can be measured if desired by detecting σ_+ and σ_- light propagating along the $\pm z$ axis instead of π and σ light as illustrated in Fig. 1.

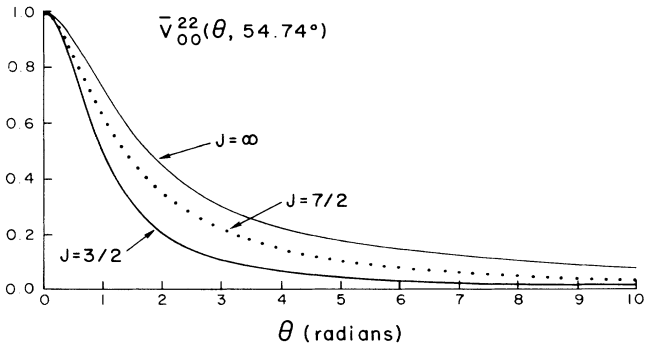

FIG. 3. The coefficient $\bar{V}^{22}_{00}$ is the mean multipole polarization T_{20} remaining after the initial multipole polarization T_{20} has been twisted by an exponential distribution of angles about a torsion axis tilted at an angle $\beta=54.7°$ from the azimuthal axis. The depolarization curves are proportional to the coefficient $\bar{V}^{22}_{00}$. Some coefficients $\bar{V}^{22}_{00}$ for levels with half-integer J are shown.

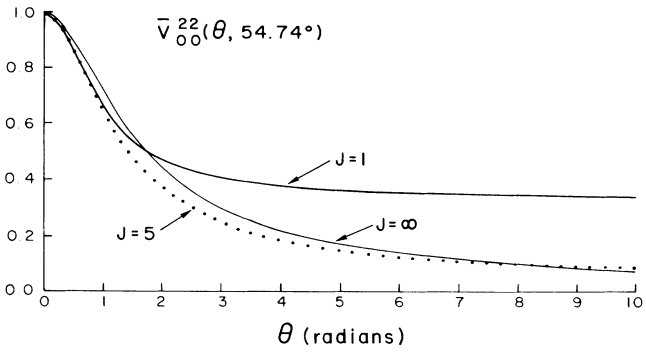

FIG. 4. Some coefficients $\bar{V}^{22}_{00}$ for levels with integer J. The baseline value is given by the parameter ϵ which is defined by (65).

The coefficients $\bar{V}^{22}_{00}$ of Figs. 3 and 4 are weighted sums of Lorentzian curves of different half-widths, in accordance with (73). For data with the usual experimental error, it is reasonable to approximate these curves with a single Lorentzian curve, i.e., we set

$$\bar{V}^{22}_{00}(\theta,54.74°)\approx\frac{1-\epsilon}{1+(\theta/\theta_{1/2})^2}+\epsilon . \tag{76}$$

The true multiple-Lorentzian coefficient $\bar{V}^{22}_{00}$ given by (73) is compared with the simple single-Lorentzian approximation (76) in Fig. 5 for $J_a=\frac{7}{2}$. Similar curves are found for other values of J_a.

We should point out here that pulsed lasers are not very reproducible in energy from pulse to pulse, so it is important to eliminate the effects of pulse-to-pulse fluctuations in the excitation efficiency. One simple way to do this is indicated in Fig. 1 where the signal ratio

$$S=\frac{S_\sigma-S_\pi}{S_\sigma+S_\pi} \tag{77}$$

is calculated. When taking this signal ratio, one must be sure that the electronic gains are adjusted to ensure that if fluorescence from unpolarized excited atoms is observed, i.e., that $S_\sigma=2S_\pi$. Since truly unpolarized excited atoms are difficult to produce, a practical way to calibrate the gains is now discussed. The atoms are excited with linearly polarized light whose polarization axis is tilted from the z axis by the "magic angle" 54.74°. Ordinary one-photon excitation or n-photon excitation can be used. The linear polarization ensures that only even multipole moments of atomic polarization excited up to a maximum

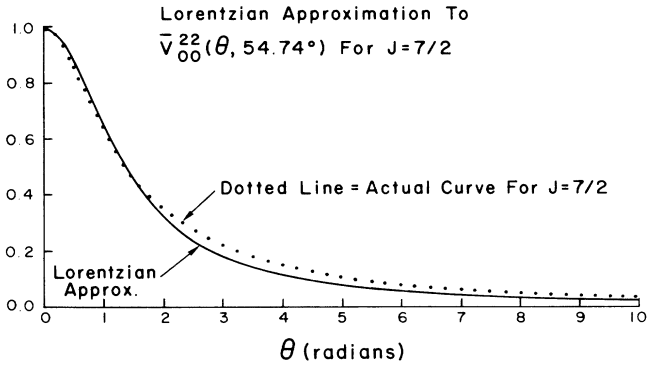

FIG. 5. A comparison of $\bar{V}^{22}_{00}$ for a level with $J=\frac{7}{2}$ and a simple Lorentzian curve of the same width. Similar curves are found for other values of J. The Lorentzian curve is a good approximation to $\bar{V}^{22}_{00}$, which is actually a superposition of Lorentzians.

multipolarity index of $L=2n$ if $J_a \geq n$ where n is the number of photons absorbed in the transition. The magic tilt angle ensures that there is no longitudinal alignment ($L=2$, $M=0$), the only type of atomic polarization which can influence the signals S_π and S_σ in Fig. 1. The electronic gains are then adjusted so that $S_\sigma = 2S_\pi$. No light shift laser should be used in the calibration step since the light shift pulse can upset the symmetry conditions needed for the calibration, but a magnetic field directed along the z axis is permissible. The predicted form of S follows from the formula (55) for the π signal and (59) for the σ signal:

$$S=\tfrac{1}{3}(1-AB\bar{V}^{22}_{00})\approx 1-AB\epsilon-\frac{AB(1-\epsilon)}{1+(F/F_{1/2})^2}\ , \tag{78}$$

where the single-Lorentzian approximation on the right of (78) follows from (76).

We shall now show how to calculate the parameters A and B which determine the signal strength. To evaluate B we note from Ref. 18 that for fluorescent light of linear polarization $\hat{\mathbf{u}}$ we may write $\mathcal{L}$ as

$$\mathcal{L}\propto\left[1-3[J_a]W(1,2,J_f,J_a;1,J_a)\left[\frac{8\pi}{15}\right]^{1/2}\times\sum_M Y_{2M}(\hat{\mathbf{u}})T^{\dagger}_{2M}\right]\ , \tag{79}$$

where W is a Racah coefficient. Comparing (79), (49), and (53), we find that

$$B(J_a,J_f)=-2\sqrt{6}[J_a]W(1,2,J_f,J_a;1,J_a)\ . \tag{80}$$

Values of B are listed in Table II for $J_a \leq 10$.

The amplitude A of the initial alignment depends on how anisotropic the initial populations $\langle m\,|\,\rho_i\,|\,m\rangle$ of the sublevels of a are. We assume that ρ_i has no off-diagonal matrix elements because of the symmetry of the excitation process, and for convenience we assume that ρ_i is normalized to unity, i.e.,

$$\sum_m \langle m\,|\,\rho_i\,|\,m\rangle = 1\ . \tag{81}$$

Then from (27) and (52), we find

TABLE II. Branching factor $B(J_a,J_f)$.

J_a	$J_f=J_a-1$	$J_f=J_a$	$J_f=J_a+1$
1	−4.899	2.450	−0.490
$\frac{3}{2}$	−4.000	3.200	−0.800
2	−3.742	3.742	−1.069
$\frac{5}{2}$	−3.666	4.190	−1.309
3	−3.666	4.583	−1.528
$\frac{7}{2}$	−3.703	4.983	−1.728
4	−3.761	5.265	−1.915
$\frac{9}{2}$	−3.830	5.571	−2.089
5	−3.906	5.858	−2.253
$\frac{11}{2}$	−3.985	6.131	−2.409
6	−4.068	6.392	−2.557
$\frac{13}{2}$	−4.151	6.642	−2.698
7	−4.235	6.882	−2.834
$\frac{15}{2}$	−4.319	7.113	−2.964
8	−4.402	7.337	−3.089
$\frac{17}{2}$	−4.485	7.554	−3.211
9	−4.568	7.765	−3.328
$\frac{19}{2}$	−4.649	7.970	−3.442
10	−4.730	8.170	−3.552
$\to\infty$	$-1.265\sqrt{J_a}$	$2.530\sqrt{J_a}$	$-1.265\sqrt{J_a}$

$$A=\mathrm{Tr}(T_{20}\rho_i)$$
$$=\sum_m \langle m\mid\rho_i\mid m\rangle C(J_a,J_a,2;m,-m)(-1)^{m-J_a} . \quad (82)$$

Using algebraic formulas for the Clebsch-Gordan coefficients we can rewrite (82) as follows:

$$A=\left[\frac{20(2J_a-2)!}{(2J_a+3)!}\right]^{1/2}\sum_m \langle m\mid\rho_i\mid m\rangle[3m^2-J_a(J_a+1)] . \quad (83)$$

We turn now to a brief discussion of the influence of a small magnetic field on the inverse hook signals. Because of the axial symmetry of the excitation process, a magnetic field along the z axis will have no effect until the light shift pulse generates transverse polarization. We have already discussed how any influence of the magnetic field after the light shift pulse can be eliminated by properly choosing the symmetry of the detection system, i.e., by observing π and σ fluorescence. During the light shift pulse, the rotation due to the magnetic field will occur simultaneously with the twist due to the light shift laser, and the Hamiltonian will be

$$H=\hbar\left[\Omega J_z+\frac{IJ_\zeta^2}{\Delta F(2J-1)}\right] , \quad (84)$$

where the Larmor frequency Ω was defined in (46), and the light intensity I and characteristic fluence ΔF were defined in (16) and (18). A term representing the scalar light shift [the parameter ϕ_0 of (18)] has been dropped from (84) since it causes no change in the atomic polarization. The unitary operator U which describes the change in atomic polarization satisfies the Schrödinger equation

$$i\hbar\frac{dU}{dt}=HU . \quad (85)$$

The solution to (85) was already given in (14) for the case of no magnetic field. Our aim here is to understand the small broadening of the inverse hook signals due to the magnetic field well enough to be sure that it is negligible. We shall consider an idealized light shift pulse which has constant intensity for the duration t_f-t_i of the pulse and has zero intensity before and after. Then the Hamiltonian H in (84) is time independent during the pulse and we may solve (85) by simple exponentiation

$$U(\psi,\theta,\beta)=\exp\left[-i\left[\psi J_z+\frac{\theta J_\zeta^2}{2J-1}\right]\right] , \quad (86)$$

where the magnetic rotation angle is

$$\psi=\Omega(t_f-t_i) \quad (87)$$

and the light shift twist angle is

$$\theta=\frac{I}{\Delta F}(t_f-t_i) . \quad (88)$$

Then (45) becomes

$$UT_{L'M'}U^\dagger=\sum_{L,M} T_{LM}W_{MM'}^{LL'} , \quad (89)$$

where U is given by (86) and

$$W_{MM'}^{LL'}(\psi,\theta,\beta)=\mathrm{Tr}(T_{LM}^\dagger UT_{L'M'}U^\dagger) . \quad (90)$$

Reviewing our previous analysis, we see that the expression (78) for the inverse hook signal remains valid if we account for the magnetic rotation during the light shift pulse by replacing the matrix element $\bar{V}_{00}^{22}$ by $\bar{W}_{00}^{22}$, the speckle averaged value of W_{00}^{22} defined by (90).

There are several important symmetry properties of W which will help us to understand the influence of a magnetic field on the inverse hook signals. Consider a rotation by 180° of the magnetic field and the light shift beam around the y axis of Fig. 1. Then $\hat{\mathbf{z}}\rightarrow-\hat{\mathbf{z}}$ and $\hat{\boldsymbol{\zeta}}\rightarrow-\hat{\boldsymbol{\zeta}}$ so the magnetic rotation caused by the rotated fields changes sign but the twist caused by the light shift remains the same. Formally, we have

$$RU(\psi,\theta,\beta)R^\dagger=U(-\psi,\theta,\beta) , \quad (91)$$

where

$$R=e^{-i\pi J_y} . \quad (92)$$

Using (91) and (90), we find the rotated matrix element to be given by

$$W_{MM'}^{LL'}(-\psi,\theta,\beta)=\mathrm{Tr}(T_{LM}^\dagger RUR^\dagger T_{L'M'}RU^\dagger R^\dagger)$$
$$=(-1)^{L+M+L'+M'}\mathrm{Tr}(T_{L,-M}^\dagger UT_{L',-M}U^\dagger) , \quad (93)$$

or

$$W_{MM'}^{LL'}(-\psi,\theta,\beta)=(-1)^{L+L'+M+M'}W(\psi,\theta,\beta) . \quad (94)$$

In (93) we have made use of the fact that

$$R^\dagger T_{LM}R=(-1)^{L+M}T_{L-M} , \quad (95)$$

which can be verified using the definition of the spherical tensor T_{LM}, cf. (28) and the following property of the rotation matrix:[17]

$$d_{M'M}^L(\pi)=(-1)^{L-M}\delta_{M,-M'} . \quad (96)$$

A second symmetry follows from the fact that

$$U(-\psi,-\theta,\beta)=U^\dagger(\psi,\theta,\beta) . \quad (97)$$

Substituting (97) into (90), we find since $T_{LM}^\dagger=(-1)^M T_{L-M}$,

$$W_{MM'}^{LL'}(-\psi,-\theta,\beta)=(-1)^{M+M'}W_{-M,-M'}^{LL'}(\psi,\theta,\beta) . \quad (98)$$

The symmetries (94) and (98) remain valid for the matrix elements $\bar{W}_{MM'}^{LL'}$ which have been averaged over a speckled distribution of twist angles [cf. (60)]. For the matrix element $\bar{W}_{00}^{22}$ which determines the shape of the inverse hook signal according to (78), the symmetries (94) and (98) imply that

$$\bar{W}_{00}^{22}(-\psi,\theta,\beta)=\bar{W}_{00}^{22}(\psi,\theta,\beta) , \quad (99)$$

$$\bar{W}_{00}^{22}(\psi,-\theta,\beta)=\bar{W}_{00}^{22}(\psi,\theta,\beta) , \quad (100)$$

i.e., $\bar{W}_{00}^{22}$ is an even function of both the mean twist angle θ and the magnetic rotation angle ψ. This implies that

the perturbation of the inverse hook signal will scale as the square of the magnetic field and will rapidly approach zero for rotation angles ψ less than unity. The twist angle for half depolarization $\theta_{1/2}$ is defined by an equation analogous to (74)

$$\overline{W}^{22}_{00}(\psi,\theta_{1/2},\beta)=\frac{1+\overline{W}^{22}_{00}(\psi,\infty,\beta)}{2} . \tag{101}$$

A plot of the half-width parameter $\theta_{1/2}$ versus ψ^2 for the case where $J_a=\frac{3}{2}$ is shown in Fig. 6.

Although we have focused the discussion of this section on the simple experimental arrangement of Fig. 1, the theory we have presented is sufficiently general to describe most experimental situations. For example, the generalization of (51) is

$$S=\sum_{L,M.L',M'}\frac{\mathcal{L}_{LM}\overline{V}^{LL'}_{MM'}\rho^*_{L'M'}}{1+iM\Omega\tau_a} , \tag{102}$$

where the components $\mathcal{L}_{LM}=\mathrm{Tr}(\mathcal{L}T_{LM})$ of the fluorescent light operator and $\rho_{L'M'}=\mathrm{Tr}(\rho T_{L'M'})$ of the initial density matrix can be found from formulas in Ref. 18.

We see that the signal as a function of fluence is always given in terms of the torsion coefficients $\overline{V}^{LL'}_{MM'}(\theta,\beta)$ which we discussed in some detail earlier. The values of the other factors in (102), $\mathcal{L}_{LM}$ and $\rho^*_{L'M'}$, determine which linear combinations of the torsion coefficients contribute to the signal. The geometrical symmetry of the experiment determines which of the coefficients $\rho^*_{L'M'}$ and $\mathcal{L}_{LM}$ are nonzero.

III. CONCLUSIONS

We have chosen to call this new method to measure oscillator strengths the "inverse hook method" because of its close connection to the conventional hook method[10] which is also used to measure oscillator strengths. The essence of the relationship is indicated in Fig. 7. In the conventional hook method atoms of a known number density N in some energy level and of a known column

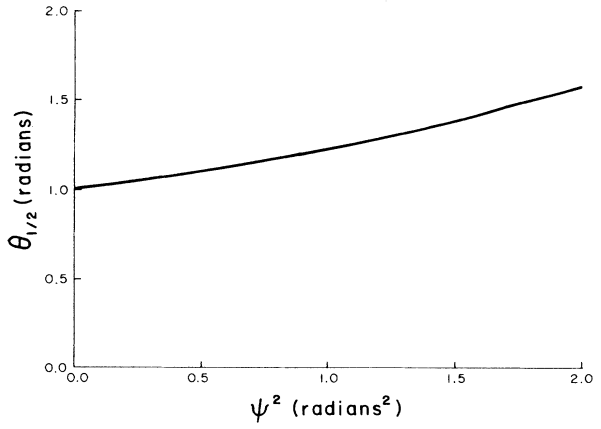

FIG. 6. Dependence of $\theta_{1/2}$, the mean twist angle for half depolarization, on ψ^2 the square of the magnetic rotation angle. Small magnetic rotation angles cause a small broadening of the depolarization curves.

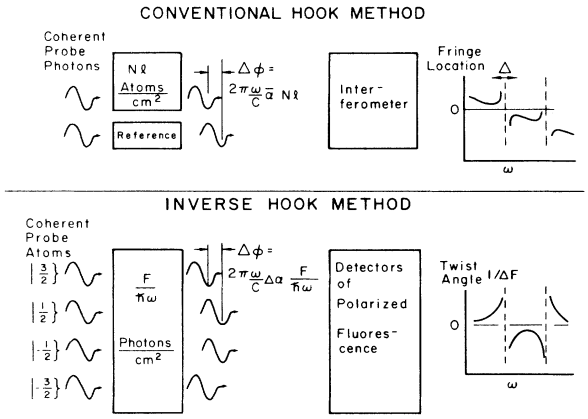

FIG. 7. Comparison of the conventional hook method and the inverse hook method. Both the conventional hook method and the inverse hook method are based on the interaction of off-resonant light with atoms. The interaction causes phase shifts between the two light beams of a conventional hook experiment, and these phase shifts are detected by an optical interferometer. In the inverse hook method the interaction causes phase shifts in the amplitudes of the $2J+1$ sublevels $|m\}$ of the atom, and these phase shifts cause the atomic polarization to twist around the direction of linear polarization of the light shift laser. The twist angle per unit fluence $1/\Delta F$ can be determined from the depolarization of the fluorescent light.

length l are traversed by one of two coherent optical beams which have been formed with a beamsplitter. The other optical beam passes through a reference path which introduces a large phase retardation. The optical phase retardation $\Delta\phi$ produced by the atoms is given by

$$\Delta\phi=2\pi\frac{\omega}{c}\bar{\alpha}Nl , \tag{103}$$

where ω is the optical frequency and $\bar{\alpha}$ is the mean atomic polarizability, i.e., $\bar{\alpha}=(1/[J_a])\sum_m\alpha(m)$. Here we have assumed the atoms are well approximated by an optically dilute gas. After passage through the atomic vapor or the reference cell, the two beams are recombined to form interference fringes. These are dispersed in optical wavelength λ with a spectrometer to form a pattern similar to that shown in Fig. 7. The large fringe displacement near atomic resonance lines due to the greatly increased polarizability together with the sloping background due to the large phase retardation of the reference path, produces "hooks" in the fringes as shown in Fig. 7. It is possible to infer the phase shift $\Delta\phi$ from the hook spacing Δ, which equals $\lambda_>-\lambda_<$ where $\lambda_>$ and $\lambda_<$ are the wavelengths on either side of the resonance wavelength where the interfernce fringes have horizontal slope. If the atomic column density Nl is known, one can use (103) to determine the oscillator strength. By appropriately choosing the amount of retardation introduced in the reference path, the hook spacing can be much larger than characteristic linewidths associated with collision or Doppler broadening. Therefore, both the hook method and inverse hook method, which uses a light shift laser detuned from the transition of interest, are relatively insensitive to the

transition line shape. The need to have fairly large and accurately known values of Nl, or more precisely $((N_a/[J_a])-(N_b/[J_b]))l$, is one of the most serious limitations of the conventional hook method when it is used to obtain oscillator strengths for transitions between excited energy levels of atoms.

For the inverse hook method one basically interchanges the roles of the atoms and photons, as indicated in Fig. 7. Instead of preparing two coherent beams of light by means of an optical beamsplitter, one prepares $2J_a+1$ coherent "beams" of excited atoms by exciting with light linearly polarized along a direction $\hat{z}$ which is tilted by an angle β from the linear polarization axis of the light shift laser. Each atomic beam is in one of the eigenstates $|m\}$ of J_ξ [cf. (9)]. These atomic beams pass through a column density $F/\hbar\omega$ of photons from the light shift laser and each beam experiences a phase shift

$$\phi(m)=2\pi\frac{\omega}{c}\alpha(m)\left[\frac{F}{\hbar\omega}\right], \tag{104}$$

where $\alpha(m)$ is the polarizability of atoms in the sublevel $|m\}$. Equations (103) and (104) are completely analogous except that in (103) a column density of atoms Nl determines a photon phase shift and in (104) a column density of photons $F/\hbar\omega$ determines an atomic phase shift. Unlike the atomic column density, the laser photon column density or the pulse fluence required in inverse hook experiments is easily measured using a pyroelectric or bolometric detector to an accuracy of a few percent. The differential atomic phase shifts cause a change in the polarization and angular distribution of fluorescent light from the excited atom. For a linearly polarized light shift laser, this is equivalent to the results of a torsion operation on the spin polarization of the excited atoms.

The depolarization curve of the inverse hook method, c.f. Fig. 5, is very reminiscent of the magnetic depolarization curve of the Hanle effect.[7] The similarity is more than superficial since both phenomena involve depolarization of excited atoms. In the Hanle effect, the atomic polarization is subject to a uniform rotation rate proportional to the magnetic field, and for a given magnetic field H, the rotation angles have an exponential distribution because of the exponential distribution of atomic lifetimes. In the inverse hook method, the atomic polarization is subject to a torsion proportional to the local fluence, and for a given mean fluence F, the torsion angles have an exponential distribution because a speckled laser beam has an exponential distribution of local fluences. The Lorentzian curves of both the Hanle effect and the inverse hook method are due to the exponential distribution of rotation angles and torsion angles, respectively. In both cases, oscillatory signals can be observed by eliminating the exponential distribution. As Dodd and Series[19] first showed, this can be done for the Hanle effect by observing, as a function of magnetic field, atoms which have rotated by a well defined angle Ωt at a time t after excitation of the atoms. For the inverse hook method this can be done by observing, as a function of a spatially uniform fluence F, atoms which have been twisted through a well-defined angle $F/\Delta F$. When using the Hanle effect, Ω is ordinarily known, so the measurement yields a mean lifetime τ corresponding to an observable rotation angle $\Omega\tau$ which half depolarizes the atoms. In the inverse hook method the fluence halfwidth $F_{1/2}$ corresponding to a known torsion angle $\theta_{1/2}=F_{1/2}/\Delta F$ is found, so the measurement yields $1/\Delta F$ which according to (19) is a measure of the oscillator strengths.

In conclusion, we shall give a summary of some of the advantages of the inverse hook method over existing methods for measuring oscillator strengths. A primary advantage is that atomic number densities need not be known. Hence, the inverse hook method is particularly well suited for measuring oscillator strengths for transitions between excited states. Even the study of transitions from a bound populated state to an autoionizing state[23] should be feasible since one does not need to observe fluorescence from the autoionizing state.

A second advantage of the new method is its use of pulsed dye lasers. The high fluence of these pulses allows the determination of small oscillator strengths, which otherwise are difficult to measure. Also since dye lasers operate throughout the visible, near-uv, and near-ir regions of the spectrum, a very large number of transitions can be studied.

An important advantage of the inverse hook method when compared to the Autler-Townes effect[12,13] which also exploits the ac Stark interaction, is it does not require a spatially uniform beam or very precise knowledge of the temporal profile of the laser pulses. In fact, a completely chaotic distribution of coherent light sources giving rise to a laser speckle pattern is an excellent practical choice. Unlike the Autler-Townes method, the laser is detuned from the transition of interest. Since the detuning can be chosen to be much larger than the Doppler width and the laser linewidth, the inverse hook method is relatively insensitive to both the transition line shape and the laser spectral profile.

Finally, we would like to emphasize the new method's experimental simplicity. The three measurements it requires, namely the detuning, the laser pulse fluence, and the integrated fluorescence decay signals, are all easily obtained. The method is less complex than the measurement of atomic lifetimes or quantum beats, since very short time resolution is not required. Hence, relatively inexpensive gated integrators rather than costly transient digitizers may be used. Its application is especially easy for anyone who uses a dye laser to excite an atomic state and then measures the state's radiative lifetime. Just by splitting the pump laser beam and pumping two dye lasers, absolute transition probabilities for each possible branch, rather than a total decay rate, can be determined.

ACKNOWLEDGMENTS

This work was part of the Ph.D. thesis of William A. van Wijngaarden. It was supported by Lawrence Livermore National Laboratory Subcontract No. 3181505. We are grateful to R. Solarz and J. Paisner for initial and continued encouragement. One of us (W.A.v.W.) would like to thank the Canadian National Research Council for their financial support.

[1]H. Nussbaumer, J. Phys. **40**, 102 (1979).
[2]R. Stern and J. Paisner, Proceedings of the First International Laser Science Conference in Dallas, Texas, 1985 (unpublished).
[3]R. W. Solarz, Lawrence Livermore Laboratory, Report No. UCID-20343 (unpublished).
[4]J. I. Davis and J. A. Paisner, Lawrence Livermore Laboratory, May, 1985 (unpublished).
[5]E. Condon and G. Shortley, *The Theory of Atomic Spectra* (Cambridge University Press, Cambridge, 1953), p. 108.
[6]E. Foster, Rep. Prog. Phys. **27**, 470 (1964).
[7]A. Corney, *Atomic and Laser Spectroscopy* (Clarendon Press, Oxfoord, 1977), p. 107.
[8]Some of the various notations for the oscillator strength for a transition from a state a to a state b are related as follows:

$$(f_{ab})_{\text{Corney}}=(f_{ab})_{\text{Foster}}=(f(b,a))_{\text{Condon and Shortley}}\ .$$

[9]M. Huber and R. Sanderman, Phys. Scr. **22**, 373 (1980).
[10]M. Huber, in *Modern Optical Methods in Gas Dynamic Research,* edited by D. Dosanjh (Plenum, New York, 1971), pp. 85–112.
[11]G. C. Bjorklund *et al.*, Appl. Phys. Lett. **29**, 729 (1976).
[12]S. Autler and C. Townes, Phys. Rev. **100**, 703 (1955).
[13]R. Loudon, *The Quantum Theory of Light,* 2nd ed. (Oxford University Press, New York, 1983), pp. 305–307.
[14]P. P. Sorokin, J. J. Wynne, and J. R. Lankhard, Appl. Phys. Lett. **22**, 342 (1973).
[15]W. A. van Wijngaarden *et al.*, Phys. Rev. Lett. **56**, 2024 (1986).
[16]The initial density matrix given by (26) only has an anisotropic distribution of atoms among the sublevels of state a, if level a has angular momentum $J_a \geq 1$. If $J_a=\frac{1}{2}$, one can use circularly polarized light to creat different populations of the sublevels $|\frac{1}{2}\rangle$ and $|-\frac{1}{2}\rangle$. Finally, oscillator strengths for transitions between levels of angular momentum 0 and 1 can be determined by choosing the $J=1$ level to be the populated level.
[17]M. E. Rose, *Elementary Theory of Angular Momenta* (Wiley, New York, 1957).
[18]R. Gupta *et al.*, Phys. Rev. A **6**, 529 (1972).
[19]Dodd J. N. and Series G. W., *Physics of Atoms and Molecules* (Plenum, New York, 1978), pp. 639–677.
[20]M. Francon, *Laser Speckle and Applications in Optics* (Academic, New York, 1979).
[21]J. C. Dainty, *Laser Speckle and Related Phenomena* (Springer-Verlag, New York, 1975).
[22]J. W. Goodman, *Statistical Optics* (Wiley, New York, 1985), pp. 347–351.
[23]U. Fano, Phys. Rev. **124**, 1866 (1961).